Chemical Engineering Journal 166 (2011) 646–651

Contents lists available at ScienceDirect

Chemical Engineering Journal

journal homepage: www.elsevier.com/locate/cej

CO_2 capture using mesoporous alumina prepared by a sol–gel process

Chao Chen, Wha-Seung Ahn*

Department of Chemical Engineering, Inha University, Incheon 402-751, Republic of Korea

ARTICLE INFO

Article history:
Received 27 September 2010
Received in revised form 8 November 2010
Accepted 8 November 2010

Keywords:
Mesoporous alumina
CO_2 adsorption
PEI impregnation

ABSTRACT

Mesoporous alumina (MA) having high surface area (812 m^2/g) and large pore volume (0.83 cm^3/g) with a narrow pore size distribution was prepared by a simple sol–gel process. The as-prepared MA was characterized by XRD, N_2 adsorption–desorption isotherms, and transmission electron microscopy (TEM). The CO_2 adsorption performance of MA was tested under both low (<1 bar) pressure using a static volumetric system and high pressure (<30 bar) conditions using a gravimetric system. MA demonstrated a CO_2 capture capacity of ca. 52 $mg/g_{adsorbent}$ at 1 bar, a value higher than that of a commercial alumina or 3-aminopropyltrimethoxysilane-grafted MCM-41. High pressure (0–30 bar) CO_2 adsorption increased in a sequence of commercial alumina < SBA-15 < zeolite 13X < MA. Static adsorption and breakthrough experiments showed that MA offers high separation efficiency for CO_2 against N_2. CO_2 desorption at different temperatures was evaluated in order to identify regeneration conditions of MA after CO_2 adsorption. PEI (polyethylenimine)-impregnated MA was also prepared and tested as a CO_2 sorbent. The hybrid sorbent material achieved higher CO_2 capture capacity (120 $mg/g_{sorbent}$) than MA alone, with a level comparable to the sorption capacities of PEI functionalized mesoporous silica materials reported to date. Both as-prepared and PEI-impregnated MA exhibited stable adsorption–desorption behaviour during 5 consecutive test cycles.

1. Introduction

At present, the discharge of CO_2 into the atmosphere by the consumption of increasing amounts of fossil fuels is believed to be causing a serious global warming problem. Accordingly, much effort has been made over the last decade to develop various chemical and physical methods for CO_2 capture and sequestration (CCS) as a means of alleviating this problem [1]. Among these approaches, porous solid adsorbents have been widely investigated as a medium for CO_2 capture, as researchers attempt to exploit their large accessible surface areas and large pore volumes.

Alumina has been widely used for catalysis and adsorption processes. It is proved by several studies dealing with the infrared spectra of CO_2 adsorbed on alumina [2–5] that there are both physical and chemical adsorption sites for CO_2 on alumina surface, but only limited research has been reported on transitional alumina or activated aluminas as CO_2 adsorbents; Rosynek studied the CO_2 adsorption on commercial γ-alumina [6]; Mao and Vannice studied CO_2 adsorption property of α-alumina [7]; and Li et al. studied the binary adsorption equilibrium of CO_2 and water vapor on activated alumina [8]. Alkali metal oxide and salts-modified alumina have also been studied for CO_2 capturing agents; Horiuchi et al. modified γ-alumina by adding basic metal oxides and studied its CO_2 adsorption performance at elevated temperatures [9]; Zou et al. studied the adsorption of CO_2 on commercial basic aluminas containing ca. 5% Na [10]; Slaugh and Willis impregnated alkali salts on commercial alumina and studied CO_2 removal after calcination of the sample at 350–800 °C [11]; and Okunev et al. studied the sorption of CO_2 from wet gases over K_2CO_3 impregnated on porous alumina [12]. These aluminas usually exhibit surface areas lower than 350–400 m^2/g, and have broad pore size distributions [13].

On the other hand, there has been no investigation of CO_2 adsorption by mesoporous alumina (MA). Compared to those transitional or activated aluminas tested for CO_2 adsorption so far, MA possesses significantly higher surface area and much narrower pore size distribution in the mesopore region [14]. Therefore, increased adsorption sites for CO_2 are expected in MA, which can lead to an improved CO_2 adsorption performance. In addition, the large pore volume and narrow pore size distribution in MA also would enable us to introduce a large amount of amine-type CO_2 capturing agent into its mesopores in a well dispersed manner, which can function as an effective hybrid type CO_2 sorbent. Various amine species are known to react with CO_2 via a carbamate formation mechanism; two molecules of amine species react with one molecule of CO_2 to form a carbamate species ($2R\text{-}NH_2 + CO_2 \rightarrow R\text{-}NH_3^+ + R\text{-}NHCOO^-$). A high quality hybrid CO_2 sorbent can be obtained if a suitable amine is chosen and introduced into the pore structure of a mesoporous material. For this purpose, we have been using

* Corresponding author. Tel.: +82 32 860 7466; fax: +82 32 872 0959.
E-mail address: whasahn@inha.ac.kr (W.-S. Ahn).

1385-8947/$ – see front matter © 2010 Elsevier B.V. All rights reserved.
doi:10.1016/j.cej.2010.11.038

PEI (polyethylenimine) as a CO_2-capturing agent, since it has a high concentration of N which can interact with CO_2 molecules. It also has a higher boiling point than other amines, making it possible to achieve enhanced thermal stability of the hybrid material. Mesoporous silica has been extensively investigated as a support material for amine species [15–22], while no work to date has considered MA functionalized with amine species for CO_2 removal. It also has yet to be determined if the adsorption sites in MA alone can provide an additional contribution to CO_2 capture (i.e., excluding the contribution by PEI).

In this work, MA having desirable textural properties (high surface area and large pore volume) was synthesized via a simple sol–gel process. This as-prepared MA was systematically evaluated as a CO_2 adsorbent, and compared against the performances of commercial alumina and amine-grafted MCM-41. PEI-loaded MA was prepared by an impregnation method and the resultant hybrid material was also investigated as a CO_2 sorbent.

2. Experimental

2.1. Synthesis of MA

MA was synthesized via a sol–gel process reported by Zhang et al. [23]. Aluminum isopropoxide (Al(i-PrO)$_3$) (41.68 g) was initially added into an alcohol solvent mixture (73.6 g ethanol and 72.2 g isopropanol) at 50 °C to obtain a milky sol. Distilled water (7.2 g) was then dropped into the mixture to promote hydrolysis of aluminum isopropoxide. The sol was subsequently stirred at room temperature for 9 h, heated in an oven at 70 °C for 24 h, followed by heating at 100 °C for 2 h. This gel was placed in an autoclave and heated at 120 °C for 12 h. Finally, the gel was washed with ethanol and dried.

2.2. PEI impregnation on MA

PEI was introduced into MA according to a procedure reported by Xu et al. [17]. The maximum amount of PEI that could be introduced into MA without exceeding the available pore volume was calculated based on the pore volume of MA (0.83 cm^3/g) and the density of PEI (1.05 g/cm^3). The resultant hybrid material was designated as PEI/MA in this work. In a typical preparation, 0.87 g PEI (Aldrich, average molecular weight of 600 by GPC, linear type, b.p. of 250 °C) was dissolved in methanol under stirring for about 15 min, after which 1 g of pretreated MA was added to the PEI/methanol solution in a glove box. The resultant slurry was continuously stirred for about 30 min and then heated at 70 °C for 16 h under reduced pressure (700 mmHg).

2.3. Amine grafting on MCM-41

MCM-41 was prepared according to the procedure reported by Beck et al. [24]. Dried MCM-41 (1.5 g) was added to 15 ml of toluene with stirring, and then 3-aminopropyltrimethoxysilane (0.92 g) was added to the mixture, stirred for 6 h at room temperature, and refluxed for 4 h at 383 K. The product was filtered and washed with ethanol and dried at 343 K under vacuum.

2.4. Characterization of the materials prepared

The XRD patterns were obtained on a Rigaku diffractometer using Cu Kα (λ = 1.54 Å) radiation. Nitrogen adsorption–desorption isotherms were measured on a Micromeritics ASAP-2000 sorptometer at liquid nitrogen temperature. The specific surface areas of samples were calculated by the BET method and the pore diameters and pore size distributions were evaluated from the desorption branch of the isotherm based on the BJH (Barrett–Joyner–Halenda) model. High-resolution TEM images were obtained on an EM-2100F model operated at 200 kV. An elemental analysis (EA) was carried out for the amine-grafted and PEI-impregnated samples.

2.5. CO_2 adsorption–desorption measurement

The ambient pressure CO_2 adsorption isotherms were obtained using a BEL adsorption instrument (BELsorp-mini). Vacuum was introduced in the pretreatment process. MA and commercial γ-alumina were pretreated at 200 °C while amine-grafted MCM-41 was pretreated at 100 °C. Adsorption experiments were carried out using ultra high purity CO_2 in a pressure range of 0–1 bar at 298 K. For MA, adsorption at 273 K was also tested. Initially, all the experimental adsorption data were fitted to the Langmuir–Freundlich equation, and then the heats of adsorption were calculated by applying the Clausius–Clapeyron equation:

$$\left[\frac{\partial \ln P}{\partial(1/T)}\right]_q = \frac{-\Delta H}{R}$$

where P is pressure, T is temperature, q is the amount adsorbed, R is the gas constant and ΔH denotes the heat of adsorption. The high pressure CO_2 adsorption isotherms were obtained using a magnetic suspension balance (Rubotherm, Germany) with in situ density measurements in a closed system. Before measuring the CO_2 adsorption capacity, the buoyancy effect was corrected in ultra high purity He. High-pressure adsorption was carried out using ultra high purity CO_2 in a pressure range of 0–30 bar at 298 K.

CO_2 desorption and adsorption/desorption cycle experiment was conducted by a TGA unit (SCINCO thermal gravimeter S-1000) connected to a gas flow panel. Helium (ultra high purity, U-Sung) was used as a purge gas in the initial activation and desorption experiments, and adsorption was carried out using ultra high purity CO_2. A feed flow rate of 30 ml/min was controlled with a MFC to the sample chamber.

The gas-separation efficiency of MA was tested by breakthrough experiments using a CO_2/N_2 (15:85, v/v) gas mixture at room temperature. For this purpose, 1 g of pretreated MA was packed into a U-type stainless-steel column, and the gas mixture was fed into the column at a flow rate of 10 ml/min. The relative amounts of the gases passing through the column were monitored on a Hiden Analytical HPR20 gas analysis system. The relative intensity of each gas component was normalized to the same level by purging gas mixtures through the bypass before they passed through the column.

3. Results and discussion

3.1. Physical properties of MA

Fig. 1 shows the XRD patterns of the MA prepared samples. The single broad diffraction peak appearing at about $2\theta = 1.5°$ in Fig. 1(a) confirms the mesoporous structure of MA. The inset of the figure is a high-resolution TEM image of MA, which shows a disordered wormhole pore structure. As shown in Fig. 1(b), after PEI impregnation, the location of the characteristic Bragg diffraction peak remained nearly constant, but the intensity of the diffraction peak decreased substantially, indicating that PEI was successfully introduced into the channels of the alumina support [17].

Fig. 2 shows the N_2 adsorption–desorption isotherms of MA and commercial γ-alumina measured at 77 K. Both samples showed type IV isotherms with hysteresis loops. As shown in the inset, the pore size distribution of MA is much narrower than that of the commercial γ-alumina. Textural properties of the MA and the commercial γ-alumina are presented in Table 1. The average pore size of MA estimated using the desorption branch of the isotherm is smaller than that of commercial γ-alumina (4.1 vs 6.6 nm); how-

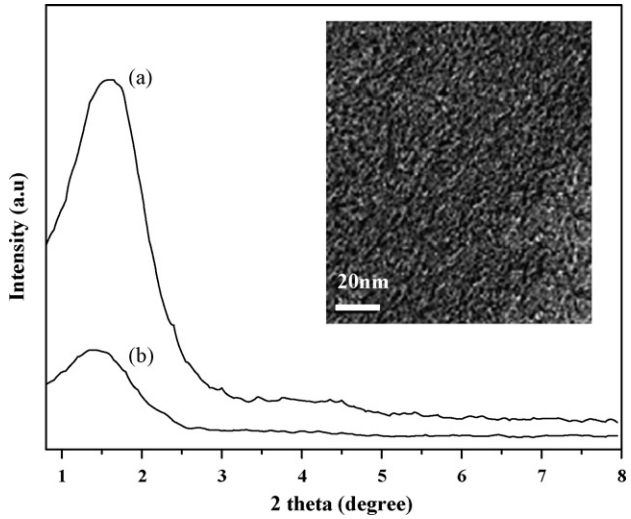

Fig. 1. XRD patterns of the MA samples prepared: (a) MA and (b) PEI/MA. The inset is the TEM image of MA.

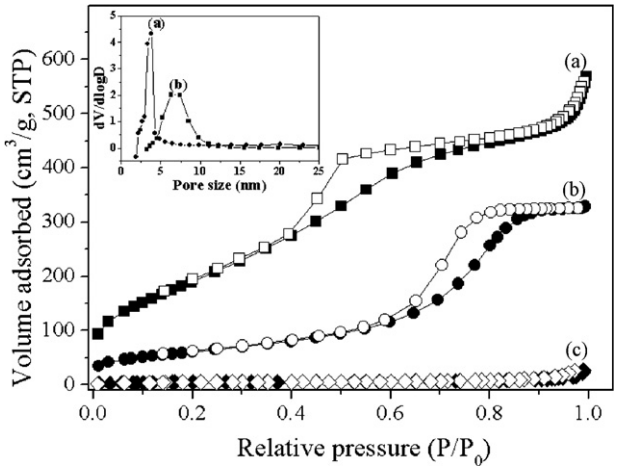

Fig. 2. N_2 adsorption–desorption isotherms: (a) MA, (b) commercial γ-alumina, and (c) PEI/MA. The insets are pore size distribution curves of (a) MA and (b) commercial γ-alumina.

ever, the surface area and pore volume of MA are substantially larger than those of commercial γ-alumina (812 vs 220 m^2/g for surface area, and 0.83 vs 0.54 cm^3/g for pore volume). These textural properties of MA are comparable to those of previously reported results for mesoporous silica materials [19]. Fig. 2(c) shows the N_2 adsorption–desorption isotherms of PEI/MA. After introducing PEI on to MA, the mesopores were virtually filled with PEI, resulting in a type II isotherm. This is consistent with the BET surface area data summarized in Table 1; the BET surface area and the residual pore volumes for PEI/MA were only 2 m^2/g and 0.03 cm^3/g, respectively.

Table 1
Textural properties of adsorbents used.

Samples	S_{BET} (m^2/g)	V_t (cm^3/g)[a]	D_p (nm)[b]
γ-Alumina	220	0.54	6.6
MA	812	0.83	4.1
PEI/MA	2	0.03	–
MCM-41	1050	0.91	2.9
SBA-15	753	1.0	5.6
Zeolite 13X	893	0.34	–

[a] Total pore volume by N_2 adsorption at $P/P_0 = 0.99$.
[b] Average pore size estimated from the desorption branch of the isotherms based on the BJH (Barrett–Joyner–Halenda) model.

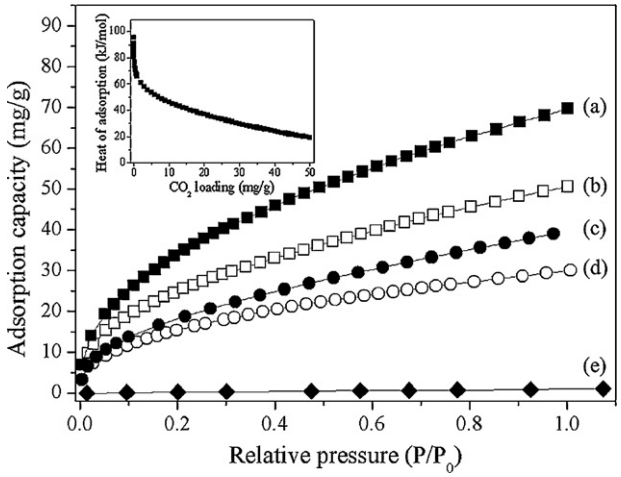

Fig. 3. CO_2 adsorption isotherms of (a) MA at 273 K, (b) MA at 298 K, (c) amine grafted MCM-41 at 298 K, (d) commercial γ-alumina at 298 K, (e) N_2 adsorption isotherm of MA at 298 K. The inset is the isosteric heat of adsorption estimated as a function of the amount of CO_2 adsorbed by MA.

3.2. CO_2 adsorption by MA

Initially, we conducted a low pressure static CO_2 adsorption experiment at 298 K. Fig. 3(b) and (d) shows the adsorption isotherms of MA and commercial γ-alumina, respectively. The adsorption capacity of MA is noticeably higher than that of commercial γ-alumina (52 vs 30 mg $CO_2/g_{adsorbent}$). This can be attributed to the high surface area of MA, which leads to more adsorption sites exposed to CO_2. We also prepared an amine-grafted mesoporous silica sample, which is well known as a CO_2 sorbent, and evaluated its sorption capacity for comparison. As shown in Fig. 3(c), 3-aminopropyltrimethoxysilane-grafted MCM-41 (N loading: 28 mg/$g_{adsorbent}$) exhibited a CO_2 sorption capacity of ca. 40 mg/$g_{adsorbent}$, which is still below the capacity of as-prepared MA. Thus, MA alone without any functionalization proved to have a significant CO_2 adsorption capacity. To have an idea about the adsorption capacities of competing adsorbents for CO_2, CO_2 capture capacities by MA in this work and other adsorbent materials reported in literature were compared in Table 2.

We further carried out CO_2 adsorption at 273 K, and the adsorption isotherm was shown in Fig. 3(a). The dependence of the heat of adsorption on the amount of CO_2 adsorbed estimated by the Clausius–Clapeyron equation is shown in the inset of Fig. 3. The heat of adsorption values decreased with increasing coverage of CO_2. As we can see, the heat of adsorption is very high at low coverage (ca. 98 kJ/mol), which is even higher than that of CO_2 chemisorption by grafted amine species (ca. 47–65 kJ/mol) [29]. High heat of adsorption values at the onset of CO_2 adsorption, i.e., at low coverage of CO_2 on the MA surface, demonstrated the chemical adsorption of CO_2 by strong adsorption sites, due to the surface hydroxyl and oxide groups, which contact with CO_2 and form bicarbonate and carbonate species [5]. Low values of heat of adsorption afterwards indicate weak physical adsorption of the CO_2 molecules. A comparison of heat of adsorption by different CO_2 adsorbents was also included in Table 2.

MA was then tested for CO_2 adsorption at high pressure conditions of up to 30 bar, and SBA-15, zeolite 13X, and commercial γ-alumina were also evaluated for comparison. Fig. 4 shows the high pressure CO_2 adsorption isotherms of these four materials. Mesoporous silica SBA-15 and commercial γ-alumina were infe-

Table 2
CO_2 capture capacities and heats of adsorption of sorbents.

Sample	Temp. (°C)	CO_2 uptake (mg/g)		ΔH (kJ/mol)	Reference
		1 bar	30 bar		
γ-Alumina	25	30	259	–	Present work
MA	25	52	381	20–98	Present work
SBA-15	25	21	260	–	Present work
Zeolite 13X	25	231	299	–	Present work
Amine-MCM-41[a]	25	40	–	–	Present work
PEI/MA	75	120	–	–	Present work
Na-ZSM-5	24	81	–	29–51	[25]
Na-Zeolite β	25	120	–	29–57	[26]
CuBTC	22	220	–	28–35	[27]
MOF508b	30	88	–	17–20	[28]
ITQ-6/AP[a]	20	53	–	22–65	[29]
APS-MCM-48[b]	25	35	–	–	[30]
TRI-PE-MCM-41[c]	25	122	–	20–92	[31]

[a] 3-Aminopropyltrimethoxysilane as amine grafting source.
[b] 3-Aminopropyltriethoxysilane as amine grafting source.
[c] 2-[2-(3-Trimethoxysilylpropylamino)ethylamino]ethylamine as amine grafting source.

rior to MA in terms of CO_2 adsorption capacity throughout the pressure range investigated. Meanwhile, zeolite 13X adsorbs more CO_2 up to ca. 10 bar, beyond which the CO_2 adsorption capacity of MA exceeds that of zeolite 13X. As pressure increases, physical properties of adsorbent such as surface area and pore volume become increasingly important for CO_2 capture, since high surface area means more adsorption sites available and large pore volume means more space for the storage of CO_2. The advantage of larger pore volume in MA becomes more evident as pressure increases, leading to a higher CO_2 capture capacity of MA than that of zeolite 13X at high pressure condition (>10 bar).

In a post-combustion CO_2 capture system, the flue gas contains a high concentration of N_2 (ca. 70%), and CO_2 separation from the CO_2/N_2 mixture should be considered. In order to evaluate the CO_2 separation efficiency of MA against N_2, we carried out experiments in both static and flow adsorption systems. As shown in Fig. 3(e), the N_2 adsorption capacity at 298 K for MA is only about 1 $mg/g_{adsorbent}$, which reflects a very high adsorption selectivity of CO_2/N_2 (52 to 1 based on the amount of each gas adsorbed at $P/P_0 = 1.0$) for MA. In a practical situation, the flue gas contains ca. 15% CO_2. Therefore, we conducted a breakthrough experiment using a gas mixture mimicking the flue gas (15% CO_2, N_2 as balance). As shown in Fig. 5, whereas N_2 appeared in the column downstream almost immediately after the process started due to a negligible adsorption capacity for N_2, no CO_2 was detected downstream of the column until ca. 160 s.

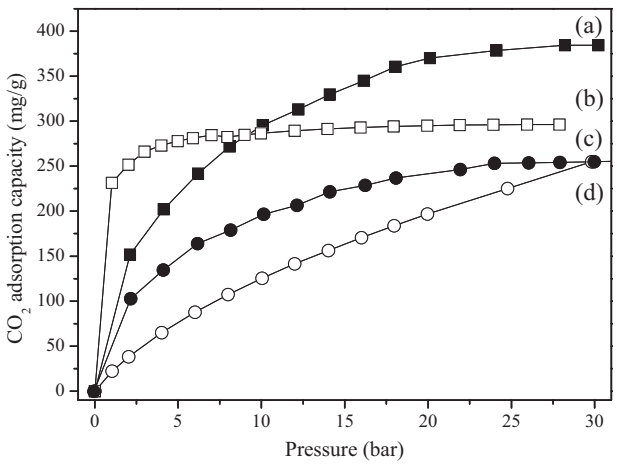

Fig. 4. High pressure CO_2 adsorption isotherms of (a) MA, (b) Zeolite 13X, (c) commercial γ-alumina, and (d) SBA-15 at 298 K.

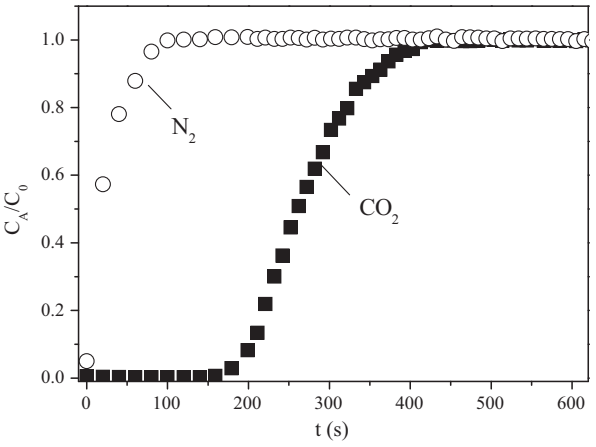

Fig. 5. Breakthrough curve of CO_2 (15% CO_2, 85% balance N_2) on MA.

In order to save energy in the system operation, the adsorbed CO_2 should be easily desorbed in an adsorbent during use of a multi-cycle adsorbent. Desorption performance of MA under a temperature swing was thus examined using a TGA unit. As shown in Fig. 6, about 60% of CO_2 can be easily desorbed at 25 °C by only a He gas purge. More than 80% CO_2 was desorbed at 100 °C and the remaining CO_2 was almost completely desorbed at 200 °C. This is consistent with the heat of adsorption values obtained above (insert in Fig. 3). CO_2 desorbed at high temperature corresponds to

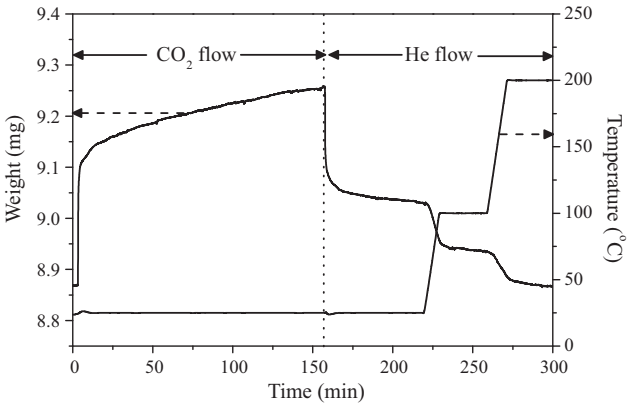

Fig. 6. CO_2 desorption behavior of MA.

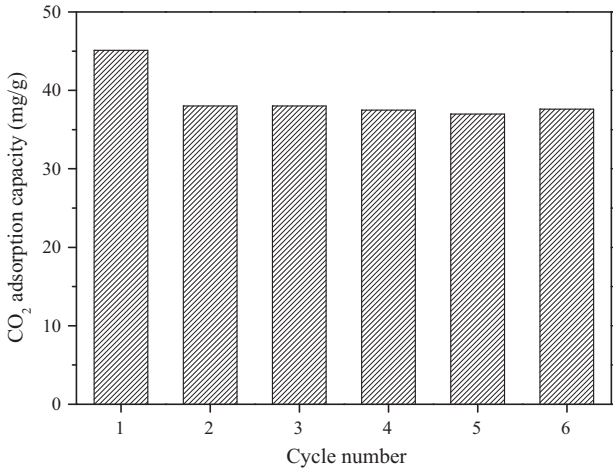

Fig. 7. Recycle runs of CO_2 by MA (adsorption at 25 °C for 150 min and desorption at 100 °C for 30 min).

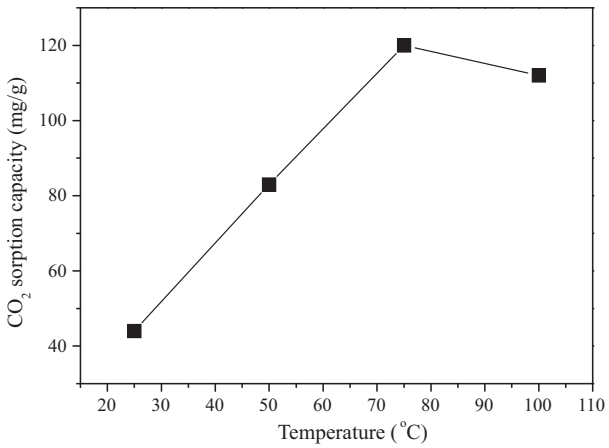

Fig. 8. CO_2 sorption performance of PEI/MA at different temperatures.

the strongly adsorbed CO_2 by the small number of strong chemical adsorption sites on the MA surface, where high heat of adsorption values were obtained, while the CO_2 desorbed at 25 °C by He gas purge indicates that most of the adsorption sites on the MA surface are weakly bound physical adsorption sites for CO_2, which corresponds to the low heat of adsorption.

Finally, the stability of MA as a CO_2 adsorbent was investigated by multiple CO_2 adsorption–desorption runs using the same TGA unit, and the results are shown in Fig. 7. We adopted 100 °C as the desorption temperature considering the marginal increase of CO_2 recovery and the high energy cost demanded at 200 °C. Full CO_2 adsorption capacity was achieved in the first cycle by the fresh MA sample. As expected, the adsorption capacity of the second adsorption step decreased compared to the initial adsorption capacity, as only ca. 80% of the captured CO_2 could be desorbed at the desorption temperature tested. Starting from the second cycle, however, MA showed virtually stable adsorption–desorption performance during 5 consecutive runs.

3.3. CO_2 sorption by PEI-impregnated MA

CO_2 capturing agent PEI was then additionally introduced to MA by an impregnation method. As reported earlier [17,19–21], the loading amount of PEI on a porous support has an important effect on the CO_2 sorption performance. In general, high loading of PEI is desirable to achieve high CO_2 sorption capacity; however, too much PEI would decrease the efficiency of the sorbent, since some PEI will be coated on the outer surface of the support and behave like a bulk phase material. Thus, the maximum allowable amount of PEI (ca. 46.5 wt%) was introduced to the pores of MA based on the pore volume of MA and the density of PEI. The resultant hybrid material was characterized by XRD (Fig. 1b) and N_2 adsorption–desorption isotherms (Fig. 2c), which confirmed the successful preparation of PEI-impregnated MA.

For this PEI-impregnated system, comparatively high temperature was needed for efficient carbon dioxide sorption. As the temperature increases, the amine groups in PEI become flexible and more CO_2-affinity sites are exposed to CO_2; the available pore space for CO_2 would also increase to some extent, leading to faster diffusion of CO_2 in the pore channels [17]. However, since the sorption process is exothermic, higher than optimal temperature favors the desorption process. Furthermore, since amine is introduced to the support by the impregnation method, the risk of amine evaporation from the support increases as the temperature is increased excessively. Therefore, initially, we investigated the effect of temperature on the CO_2 capturing capacity to determine the optimum temperature for this system. As shown in Fig. 8, CO_2 capturing capacity increased with temperature and the highest CO_2 sorption capacity (120 $mg/g_{sorbent}$) was established at 75 °C, which coincides with the optimum temperature reported by several researchers using PEI-impregnated mesoporous silica [17,19,21]. This CO_2 sorption capacity (120 $mg/g_{sorbent}$) measured is comparable to that of the PEI-impregnated mesoporous silica previously reported [17]. The N amount in the PEI-impregnated MA sample was measured to be 157 $mg/g_{sorbent}$ by an EA, and the CO_2/N ratio achieved was calculated to be 0.24. Compared to the stoichiometric CO_2/N value of 0.5 in carbamate complex formation and the average value of CO_2/N reported in an amine-grafted system on mesoporous silica [22], the CO_2/N in PEI/MA appears to be lower. However, since the total amount of amine introduced by the PEI-impregnation method is far greater than that of an amine-grafted system, higher overall CO_2 capture capacity than that of an amine-grafted system can be produced.

The cyclic performance of PEI/MA is the most important criterion to determine whether MA can be a suitable support material for PEI. Thus, the performance of the PEI/MA in 5 consecutive CO_2 sorption-desorption runs was tested in terms of its stability. Both sorption and desorption runs were carried out at 75 °C [19–21]. As shown in Fig. 9, the PEI/MA demonstrated reversible and stable CO_2 sorption–desorption performance during 5 repeated runs without deterioration of the CO_2 capturing performance.

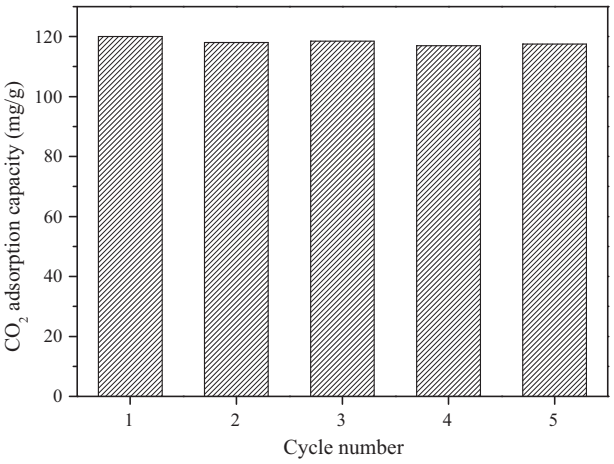

Fig. 9. Recycle runs of CO_2 by PEI/MA (adsorption at 75 °C for 150 min and desorption at 75 °C for 150 min).

The cyclic performance data of the PEI/MA indicate that MA here functions solely as a support material. After impregnating PEI into the MA, the mesopore channels are virtually filled with PEI, which was confirmed by the surface area (only 2 m^2/g) and the residual pore volume (only 0.03 cm^3/g) for the resultant hybrid material, as shown in Table 1. Thus, the CO_2 sorption process would be governed by the reaction of amine species with CO_2. The contribution of adsorption sites in MA for CO_2 capture can be neglected in PEI/MA. Otherwise, the CO_2 would not be desorbed successfully at 75 °C (see Fig. 6).

4. Conclusions

In summary, mesoporous alumina (MA) having high surface area and large pore volume was successfully synthesized by a simple sol–gel process. As-prepared MA alone showed a significant CO_2 adsorption capacity, and high adsorption selectivity of CO_2/N_2. MA maintained good stability in 5 adsorption–desorption runs. PEI-impregnated MA achieved high CO_2 sorption capacity and again performed satisfactorily during 5 consecutive adsorption–desorption test cycles, showing no deterioration. These results demonstrate that MA can be either directly used as a CO_2 adsorbent or as a support material for CO_2 sorption agents for the removal and recovery of CO_2 from power station flue gas.

Acknowledgment

This work was supported by the Carbon Dioxide Reduction & Sequestration R&D Center (CDRS), one of the 21st Century Frontier R&D Programs in Korea.

References

[1] J.D. Figueroa, T. Fout, S. Plasynski, H. McIlvried, R.D. Srivastava, Advances in CO2 capture technology? The U.S. department of energy's carbon sequestration program, Int. J. Greenhouse Gas control 2 (2008) 9–20.
[2] S.J. Gregg, J.D.F. Ramsay, A study of the adsorption of carbon dioxide by alumina using infrared and isotherm measurements, J. Phys. Chem. 73 (1969) 1243–1247.
[3] N.D. Parkyns, The surface properties of metal oxides. Part II. An infrared study of the adsorption of carbon dioxide on γ-alumina, J. Chem. Soc. A (1969) 410–417.
[4] J.B. Peri, Infrared study of adsorption of carbon dioxide, hydrogen chloride, and other molecules on "acid" sites on dry silica-alumina and γ-alumina, J. Phys. Chem. 70 (1966) 3168–3179.
[5] N.D. Parkyns, The influence of thermal pretreatment on the infrared spectrum of carbon dioxide adsorbed on alumina, J. Phys. Chem. 75 (1971) 526–531.
[6] M.P. Rosynek, Isotherms and energetics of carbon dioxide adsorption on γ-alumina at 100 °C–300 °C, J. Phys. Chem. 79 (1975) 1280–1284.
[7] C.F. Mao, M.A. Vannice, High surface area α-alumina. Adsorption properties and heats of adsorption of carbon monoxide, carbon dioxide, and ethylene, Appl. Catal. A: Gen. 111 (1994) 151–173.
[8] G. Li, P. Xiao, P. Webley, Binary adsorption equilibrium of carbon dioxide and water vapor on activated alumina, Langmuir 25 (18) (2009) 10666–10675.
[9] T. Horiuchi, H. Hidaka, T. Fukui, Y. Kubo, M. Horio, K. Suzuki, T. Mori, Effect of added basic metal oxides on CO_2 adsorption on alumina at elevated temperatures, Appl. Catal. A: Gen. 167 (1998) 195–202.
[10] Y. Zou, M. Vera, E.R. Alirio, Adsorption of carbon dioxide on basic alumina at high temperatures, J. Chem. Eng. Data 45 (6) (2000) 1093–1095.
[11] L.H. Slaugh, C.L. Willis, CO_2 removal from gaseous streams, U.S. Patent 4,433,981.
[12] A.G. Okunev, V.E. Sharonov, Y.I. Aristov, V.N. Parmon, Sorption of carbon dioxide from wet gases by K_2CO_3-in-porous matrix: influence of the matrix nature, React. Kinet. Catal. Lett. 71 (2) (2000) 355–362.
[13] J. Cejka, Organized mesoporous alumina: synthesis, structure and potential in catalysis, Appl. Catal. A 254 (2003) 327–338.
[14] C.M. Alvarez, N. Zilkova, J.P. Pariente, J. Cejka, Synthesis, characterization and catalytic applications of organized mesoporous aluminas, Catal. Rev. 50 (2008) 222–286.
[15] V. Zelenak, M. Badanicova, D. Halamova, J. Cejka, A. Zukal, N. Murafa, G. Goerigk, Amine-modified ordered mesoporous silica: effect of pore size on carbon dioxide capture, Chem. Eng. J. 144 (2008) 336–342.
[16] G.P. Knowles, S.W. Delaney, A.L. Chaffee, Diethylenetriamine[propyl(silyl)]-functionalized (DT) mesoporous silicas as CO_2 adsorbents, Ind. Eng. Chem. Res. 45 (2006) 2626–2633.
[17] X. Xu, C. Song, J.M. Andresen, B.G. Miller, A.W. Scaroni, Preparation and characterization of novel CO_2 "molecular basket" adsorbents based on polymer-modified mesoporous molecular sieve MCM-41, Micropor. Mesopor. Mater. 62 (2003) 29–45.
[18] M.B. Yue, Y. Chun, Y. Cao, X. Dong, J.H. Zhu, CO_2 capture by as-prepared SBA-15 with an occluded organic template, Adv. Funct. Mater. 16 (2006) 1717–1722.
[19] W.J. Son, J.S. Choi, W.S. Ahn, Adsorptive removal of carbon dioxide using polyethyleneimine-loaded mesoporous silica materials, Micropor. Mesopor. Mater. 113 (2008) 31–40.
[20] C. Chen, W.J. Son, K.S. You, J.W. Ahn, W.S. Ahn, Carbon dioxide capture using amine-impregnated HMS having textural mesoporosity, Chem. Eng. J. 161 (2010) 46–52.
[21] C. Chen, S.T. Yang, W.S. Ahn, R. Ryoo, Amine-impregnated silica monolith with a hierarchical pore structure: enhancement of CO_2 capture capacity, Chem. Commun. (2009) 3627–3629.
[22] P.J.E. Halick, A. Sayari, Applications of pore-expanded mesoporous silica. 5. Triamine grafted material with exceptional CO_2 dynamic and equilibrium adsorption performance, Ind. Eng. Chem. Res. 46 (2007) 446–458.
[23] Z.X. Zhang, P. Bai, B. Xu, Z.F. Yan, Synthesis of mesoporous alumina TUD-1 with high thermostability, J. Porous Mater. 13 (2006) 245–250.
[24] J.S. Beck, J.C. Vartuli, W.J. Roth, M.E. Leonowicz, C.T. Kresge, K.D. Schmitt, C.T.W. Chu, D.H.E. Qlson, W. Sheppard, S.B.J. McCullen, B. Higgins, J.L.J. Schlenker, A new family of mesoporous molecular sieves prepared with liquid crystal templates, J. Am. Chem. Soc. 114 (1992) 10834–10843.
[25] J.A. Dunne, M. Rao, S. Sircar, R.J. Gorte, A.L. Myers, Calorimetric heats of adsorption and adsorption isotherms. 2. O_2, N_2, Ar, CO_2, CH_4, C_2H_6 and SF_6 on NaX, H-ZSM-5, and Na-ZSM-5 Zeolites, Langmuir 12 (1996) 5896–5904.
[26] S.T Yang, J. Kim, W.S. Ahn, CO_2 adsorption over ion-exchanged zeolite beta with alkali and alkaline earth metal ions, Micropor. Mesopor. Mater. 135 (2010) 90–94.
[27] Q.M. Wang, D. Shen, M. Bulow, M.L. Lau, S. Deng, F.R. Fitch, N.O. Lemcoff, J. Semanscin, Metallo-organic molecular sieve for gas separation and purification, Micropor. Mesopor. Mater. 55 (2002) 217–230.
[28] L. Bastin, P.S. Barcia, E.J. Hurtado, J.A.C. Silva, A.E. Rodrigues, B. Chen, A microporous metal-organic framework for separation of CO_2/N_2 and CO_2/CH_4 by fixed-bed adsorption, J. Phys. Chem. C 112 (2008) 1575–1581.
[29] A. Zukal, I. Dominguez, J. Mayerov, J. Cejka, Functionalization of delaminated zeolite ITQ-6 for the adsorption of carbon dioxide, Langmuir 25 (17) (2009) 10314–10321.
[30] S. Kim, J. Ida, V.V. Guliants, J.Y.S. Lin, Tailoring pore properties of MCM-48 silica for selective adsorption of CO_2, J. Phys. Chem. B 109 (2005) 6287–6293.
[31] R.S. Guerrero, Y. Belmabkhout, A. Sayari, Modeling CO_2 adsorption on amine-functionalized mesoporous silica: 1. A semi-empirical equilibrium model, Chem. Eng. J. 161 (2010) 173–181.